Heliyon 9 (2023) e21977

Contents lists available at ScienceDirect

Heliyon

journal homepage: www.cell.com/heliyon

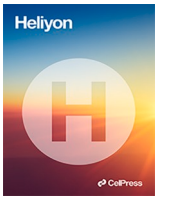

Application of Taguchi method, response surface methodology, DFT calculation and molecular dynamics simulation into the removal of orange G and crystal violet by treated biomass

Abdelkader Dabagh [a,*], Ridouan Benhiti [a], Mohamed EL-Habacha [a], Abdeljalil Ait Ichou [a,**], M'hamed Abali [a], Abdallah Assouani [a], Mahmoudy Guellaa [a], Avni Berisha [b], Rachid Hsissou [c], Fouad Sinan [a], Mohamed Zerbet [a]

[a] *Laboratory LACAPE, Faculty of Science, Ibn Zohr University, BP. 8106, Hay Dakhla, Agadir, Morocco*
[b] *Department of Chemistry, Faculty of Natural and Mathematics Science, University of Prishtina, 10000, Prishtina, Republic of Kosovo*
[c] *Laboratory of Organic Chemistry, Bioorganic and Environment, Chemistry Department, Faculty of Sciences, Chouaib Doukkali University, BP 20, 24000, El Jadida, Morocco*

ARTICLE INFO

Keywords:
Adsorption
Dye
Taguchi experimental design (TED)
Response surface methodology (RSM)
Monte Carlo simulations
Molecular dynamics (MD)

ABSTRACT

In this work, the efficiency of the treated plant *Carpobrotus edulis* (TPCE) as an effective biosorbent for removing the orange G (OG) and crystal violet (CV) dyes from aqueous solution was investigated. TPCE was characterized by FT-IR, S_s, pH_z and SEM-EDX. The influence of parameters such as bioadsorbent dose, contact time, initial concentration, temperature and pH was tested using Taguchi experimental design (TED) with L_8 orthogonal array (five parameters in two levels). The initial concentration, bioadsorbent dose and contact time are the main parameters for the removal of CV and OG dyes, while the effects of pH and temperature are minimal. The maximum removal efficiency of dyes under optimal operating conditions was 97.93 % and 92.68 %, respectively. which at the optimal conditions of 3 g/L, pH 10, 20 mg/L, 35 °C, 5 min and 15 g/L, pH 4, 20 mg/L, 35 °C, 60 min for CV and OG dyes, respectively. The results of response surface methodology (RSM) and analysis of variance (ANOVA) showed that the initial concentration C_i of CV dye was the most significant factor in the adsorption efficiency with a contribution of 51.56 %. On the other hand, the OG bioadsorbent dose is the most important factor in adsorption efficiency with a percentage contribution of 56.41 %. The Density Functional Tight Binding (DFTB) method shows that dyes strongly bind the adsorbent surface. Monte Carlo and molecular dynamics simulations show significant interactions between dye and adsorbent surface. The reusability of biomaterial indicated that the adsorption performance dropped very slightly up to five cycles.

1. Introduction

Crystal violet (CV), as one of the toxic cationic dyes, is considered a practical and common dye in many industrial fields (textiles, pharmaceuticals …), but is also considered a difficult compound to manipulate due to its non-biodegradability. CV has carcinogenic,

* Corresponding author.
** Corresponding author.
E-mail addresses: abdelkader.dabagh@gmail.com (A. Dabagh), aitichou.contact@gmail.com (A. Ait Ichou).

https://doi.org/10.1016/j.heliyon.2023.e21977
Received 25 August 2023; Received in revised form 27 October 2023; Accepted 1 November 2023
Available online 7 November 2023

mutagenic and harmful effects on humans [1,2]. CV in the body causes fatal diseases such as hypermobility, abdominal pain and respiratory diseases [3]. Orange G (OG) is an anionic dye, a very toxic, mutagenic, carcinogenic and pathogenic compound used in various industrial sectors such as wool and fiber, paper, leather, etc., and is banned for cosmetic and pharmaceutical products due to its toxicological profile [4,5].

Unfortunately, many industries dump their polluted water into the oceans or lakes, leading to groundwater and surface water contamination. Researchers around the world are trying to combat environmental pollution. Therefore, the issue of removing dyes from water sources remains one of the most important issues, especially in recent years. Some methods are widely used, such as nanofiltration, reverse osmosis [6], coagulation–flocculation [7], oxidative degradation [8–10], hybrid treatments [11] and membrane filtration [12]. However, among all these techniques, many researchers generally prefer adsorption as a simple and inexpensive process.

In addition to the most commonly used sorbents, namely zeolite [13], activated carbon [14,15], and newly synthesized composites [16–19], biomaterials, which represent an ecological and environmentally friendly option, have recently been presented as cost-effective and efficient adsorption of harmful dyes in aqueous solutions [20–22]. In this work, the plant *C. edulis* was used as an adsorbent to remove CV and OG dyes from an aqueous solution. The choice of these carriers is based on their abundance, non-toxicity, ease of preparation and low cost, also in combination with a variety of functional groups that can fix the dyes, including hemicelluloses, lipids or lignin [23,24]. On the other hand, chemical modification of these plants by chemical agents allows increasing the efficiency of dye adsorption, and in this category, pretreatment with an acid or base was the most common modification method [25].

The factors and experiences that influence the process are each realized in the form of a factor. In this methodology, the different parameters are realized by changing the actual parameter under study at different levels while leaving other parameters unchanged. The experiments are repeated for all parameters, which significantly increases the number of experiments to achieve optimal conditions using this approach. To overcome these obstacles, various experimental design methods based on statistical and mathematical approaches have been developed, such as Taguchi Experimental Design (TED) and Response Surface Methodology (RSM) [26–28]. The influence of parameters on the response could be determined using the Taguchi method with an experimental design approach; in addition, optimal process conditions could be achieved with TED. This method provides optimal conditions with a minimum number of experiments with orthogonal arrays, thereby reducing costs. The RSM method is most useful for designing experiments and analyzing the results to draw a meaningful and robust conclusion. The RSM method is a specialized collection of mathematical and statistical techniques used to design experiments, estimate optimal conditions, build models, determine the effects of independent parameters on dependent parameters, and achieve optimal conditions for multiple responses in parallel. Furthermore, the graphs created by the RSM approach are three-dimensional, so the evolution of all parameters can be represented in a single graph [29,30].

The extensive use of organic dyes has led to their widespread occurrence in the environment, which has been recognized as a potential threat to human health and aquatic ecosystems. Because there are scientific and societal concerns about the impacts of these emerging pollutants, there is a need to better understand their effective removal from the environment. However, studying the complex interactions between these dyes and sorbents at the molecular level presents significant challenges.

This article focuses on the experimental design to optimize the adsorption of dyes of triphenylmethane (CV) and diazo (OG) classes on the biomaterial based on the plant *Carpobrutus edulis* modified by alkaline treatment (TPCE) using TED and RSM. The main parameters affecting the removal efficiency were selected as control factors: bioadsorbent ratio, contact time, initial concentration, temperature and pH. A linear mathematical model was created to illustrate the effects of the various factors and their interactions. These include the main effect for each parameter, the normal probability of residuals, analysis of variance (ANOVA), effects and interactions between the operating parameters. Furthermore, we investigated the properties of treated plants as biosorbents with properties to understand the adsorption mechanism and dynamic behavior of the orange G and crystal violet dyes. To consider various

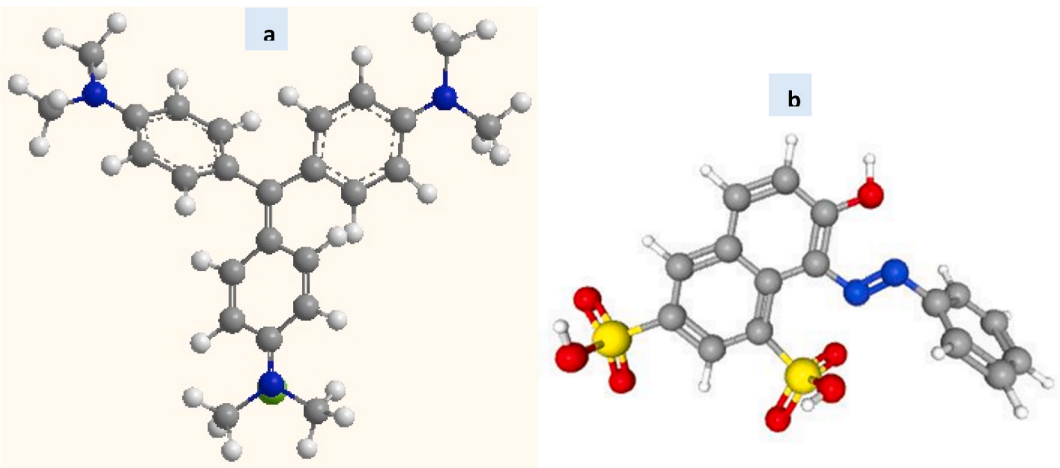

Fig. 1. Structural formulae of the dyes: (a) Crystal Violet, (b) and Orange G (C = grey, H = white, N = blue, Cl = green, O = red, Na = dark grey, S = yellow). (For interpretation of the references to colour in this figure legend, the reader is referred to the Web version of this article.)

critical aspects such as the influence of different adsorption sites, the adsorption energetics and the underlying mechanism, we used the Density Tight Binding Functional Theory (DFTB+) approach, Monte Carlo simulations and Molecular Dynamics (MD) simulations.

2. Materials and method

2.1. Preparation of dyes solutions

All agents employed in this work were of the purest analytical quality and were purchased from Sigma Aldrich. The cationic dye Crystal Violet (molecular formula $C_{25}N_3H_{30}Cl$, MW: 407.98 g/mol, λ_{max} of 580 nm, and the molecular dimension of the CV: (length) = 11.37 Å; (width) = 10.25 Å) and Orange G (molecular formula C_{16} H_{10} $N_2Na_2O_7S_2$, MW: 452.38 g/mol, and λ_{max} of 476 nm, and the molecular dimension of the OG: (length) = 13.8 Å; (width) = 8.3 Å) as an example of a toxic anionic dye, were removed from the aqueous solution. The pH of the solution was monitored with 0.1 M of hydrochloric acid and sodium hydroxide. Double distilled water was used to prepare all solutions. The structures of CV and OG are shown in (Fig. 1a and b).

2.2. Preparation of biosorbent

The native plant *Carpobrotus edulis* (NCE) was collected in the Souss-Massa region (Morocco). The aim of the chemical treatment of biomaterials is, on the one hand, to activate and increase the adsorption capacity by removing particles that naturally adhere to ion exchange surfaces, such as trace elements (calcium, sodium), and on the other hand, elimination of as many soluble chemical elements as possible (soluble organic substance) in aqueous solutions. NaOH-modified *Carpobrotus edulis* plant (TPCE) was prepared by shaking particles of *C. edulis* plant (100 g) in 0.1 N NaOH solution at ambient temperature for 8 h. The biomaterial was then gently washed with distilled water until the pH became neutral, and then the treated material was dried at 60 °C for 72 h. The biomaterial was crushed and passed through a (<250 μm) mesh sieve, and then stored in a desiccator for the remainder of this work.

2.3. Adsorption experiment

The batch adsorption capacity of the treated plant was tested by modifying physical parameters such as bioadsorbent ratio, pH, temperature, initial concentration and contact time. A Defined mass of adsorbent was weighed and placed in an Erlenmeyer flask (100 mL) with 40 mL of dye solution of a defined concentration (CV or OG). The solutions were stirred for sufficient time to reach equilibrium and then centrifuged at 3000 rpm for 5 min. The concentration of the different dyes in the aqueous solution was calculated using a UV–Vis spectrophotometer (Jasco V-630 UV/Vis spectrophotometer). The wavelengths of the adsorption maximum are 580 and 476 nm for crystal violet and orange G, respectively.

The response R (%) is the percentage of adsorption of the dyes by the selected biomaterial according to the following formula (Eq. (1))

$$\%Removal = \frac{(C_i - C_e)}{C_i} \times 100 \quad (1)$$

C_0 and C_e are the initial and equilibrium concentrations (mg/L), respectively, of the relevant dyes.

2.4. Modeling and experimental designs

2.4.1. Taguchi experimental design (TED)

The Taguchi method brings a significant improvement to full and partial factorial designs by significantly reducing the number of trials while maintaining good accuracy. This method provides insights that lead to the optimization of the system under investigation. It allows determining the optimal values of the different parameters that control the process and identifying the most influential factors, the possible interactions between the factors and the minimum number of measurement points to obtain maximum information [31,32].

To carry out this work, we used MINITAB software, which facilitates the creation and interpretation of data. The experiments were performed randomly, with a lower and a higher level for each parameter. Using a statistical analysis of variance, the concept was validate and the percentage contribution of the various factors to the adsorption efficiency was calculated. This Taguchi method was

Table 1
Coded parameters and experimental values for the removal of dyes using TED.

parameters	Symbols	Ranges and levels	
		Low (−1)	High (+1)
Bioadsorbent ratio *(g/L)*	**R**	3	15
Contact time *(min)*	$\mathbf{t_c}$	5	60
Initial concentration *(mg/L)*	$\mathbf{C_i}$	20	200
pH	pH	4	10
Temperature *(°C)*	**T**	18	35

based on 8 adsorption experiments as shown in Table 1.

2.4.2. Response surface methodology

The RSM is used extensively for optimization and development in numerous disciplines, particularly in chemistry. RSM is a holistic method that, based on the comparison of empirical models and experimental test results, takes into account the effects of individual factors, their combination and interactions on the process, thus enabling successful prediction and optimization of the specific process [33,34]. In general, a linear empirical model is applied to accurately describe the dependence of the response on certain independent parameters. Independent variables include large effects, higher-order main parameters, and higher-order bidirectional interactions between parameters. The RSM is generally used in the Box-Behnken design.

2.5. Computational details

2.5.1. DFTB+

For all density functional-based tight binding (DFTB) calculations, we used the software tool DFTB + [35–38]. DFTB+ is a comprehensive open source software suite designed for efficient and fast atomistic quantum mechanical simulations. It enables the simulation of large systems and long time scales with reasonable accuracy and offers significant speed advantages over traditional ab initio methods [35,36]. DFTB + includes various approximations of density functional theory (DFT), including DFTB and the extended tight binding method. DFTB is particularly suitable for the simulation of organic matter, insulators, solids, clusters, semiconductors, metals and even biological systems as it provides an efficient and accurate approach [39]. In our study, we used the 3OB-Koster library set [36] to evaluate the potential interactions between atoms. The convergence tolerance for energy was set to 0.01 kcal/mol, while the force tolerance was set to 0.1 kcal/mol. Additionally, the displacement tolerance was set to 0.001. To provide a visual representation of the adsorbent model, Fig. 2 illustrates its structure. The model size was: 7 × 7 (composed of: 126C and 30H atoms) graphene layer to accommodate the CV or OG molecules (adsorbates) [40].

The interaction energy, both, in vacuum is evaluated as follow [40–48]:

$$E_{interaction} = E_{CV\ or\ GO/Adsorbent} - (E_{CV\ or\ GO} + E_{Adsorbent})$$

where $E_{Adsorbent/CV\ or\ OG}$ is the total energy of the adsorption system. $E_{Adsorbent}$ and $E_{CV\ or\ GO}$ are the energies of the isolated CV or GO and adsorbent respectively.

2.5.2. Monte Carlo and molecular dynamic

We used Monte Carlo (MC) simulations to investigate the interaction between CV and OG and the modeled biomaterial surface within the simulated adsorption environment. The MC calculations included the biomaterial surface, one sofosbuvir molecule, and one thousand water molecules. For these simulations, we used the COMPASSII force field [49], which is known for its precision and reliability in MC calculations.

To further investigate the system dynamics, molecular dynamics (MD) simulations were performed under the NVT ensemble at 298 K [44,46,50–52]. The Total simulation time was 0.8 ns (ns) for MD experiments [51–56]. This allowed us to observe the behavior and movement of the molecules within the system over a longer period of time, and provide information about their interactions and the entire adsorption process.

3. Results and discussion

3.1. Characteristics of biadsorbent

As mentioned in our previous work [57], detailed characterization of *C. edulis* plant in native and treated states was carried out using different techniques.

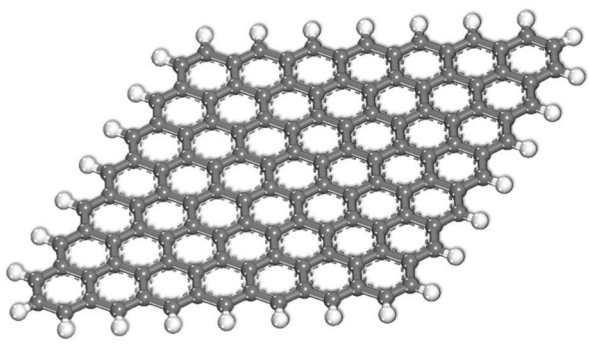

Fig. 2. Optimized structure of the adsorbent model used for theoretical DFTB + calculations.

The plant treated with the chemical agent NaOH shows that after treatment the pores have a larger volume and a greater variety of porosity and micropore size, which confirms a large surface area and therefore allows a better adsorption possibility of the dyes in these pores, confirmed the surface modification of the studied biomaterial after treatment (Fig. 3a).

To determine the chemical elements present in the biomaterial, elemental analysis was performed (Fig. 3 b, Table 2). The data indicate the significant presence of carbon and oxygen, which are the main elements of the biomaterial. While the native *C. edulis* plant (NCE) is characterized by its high content of sodium, chloride, potassium and calcium elements. Basic treatment of this plant removes all sodium, chloride, potassium and calcium elements. The release of K^+, Ca^{2+} and Na^+ would facilitate the adsorption of CV, which is characterized by a cationic nitrogen group (N). The release of Cl^-, on the other hand, would facilitate the adsorption of the OG dye, which is characterized by two anionic sulfonate groups.

The FT-IR spectrum of the plant in the treated state is shown in Fig. 3 c. The biomaterial indicates the peak at 3400 cm^{-1} referring to the OH stretching vibration. The peak at 2900 cm^{-1} refers to the C–H stretching vibration. The bands at 1600 cm^{-1} relate to the valence vibrations of the carboxyl groups. The band lies between 1050 cm^{-1} and 1320 cm^{-1} attributed to the alcohol and amine (NH) vibrations.

The pH_z of *C. edulis* plant slightly decreased from pH_z 7.6 to 7 after NaOH treatment, which resulted in a shift in the adsorption range of cationic species such as CV dye to lower pH values. Therefore, at a pH value above pH_z, the surface of the biomaterial is negatively charged, which favors the adsorption of cationic substances, while at pH < pH_z the surface is positively charged and repels cationic substances.

Basic treatment of the *C. edulis* plant (NCE) results in a significant increase, almost a doubling of the surface area value (S_S) (Table 2). This treatment removed the mineral elements and soluble tannins present in the bioadsorbent, resulting in an increase in porosity and specific surface area.

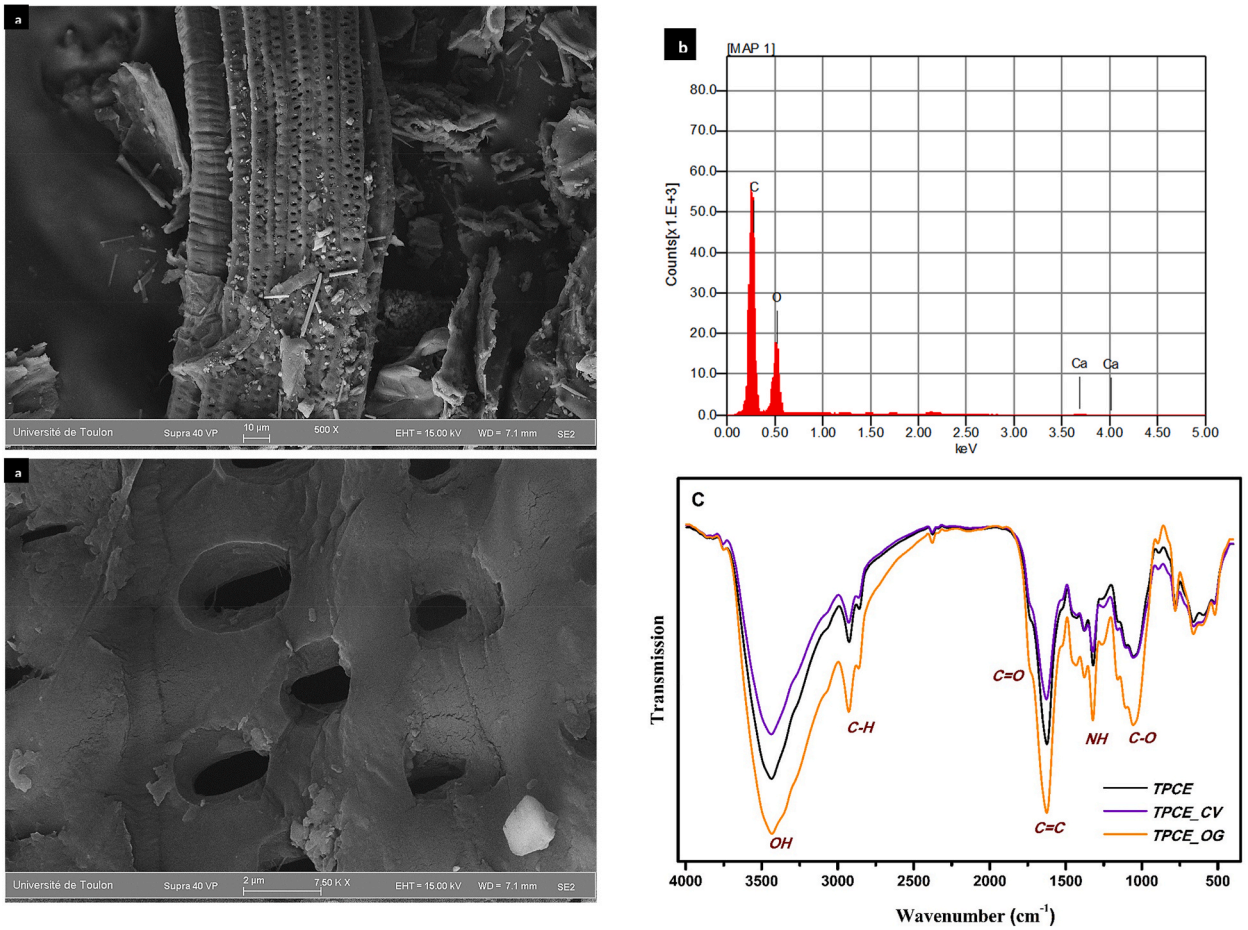

Fig. 3. (a) SEM images, (b) EDX analysis, and (c) The FT-IR spectrum of TPCE biomaterial.

Table 2
Main characteristic of bioadsorbents [58].

	Specific surface area (m^2/g)	pH_z	Elemental analysis (wt %)					
			C	O	Na	Cl	K	Ca
NCE	8.86	7.6	42.74	36.71	8.28	8.28	1.17	2.83
TPCE	19.45	7	62.10	37.23	–	–	–	0.67

3.2. Optimization using TED and RSM studies

3.2.1. Results of the tests performed

The adsorption performance (R%) of each combination was defined as a response and measured using the experimental protocol. The control factors are bioadsorbent ratio (R), contact time (t_c), initial concentration (C_i), temperature (T) and pH. The values of the different experiments are summarized in Table 3.

3.2.2. Influences and interactions between factors (analysis of variance (ANOVA)

The parameters affecting dye elimination were identified by conducting an analysis of variance (Table 4). In this approach, the sum of squares of each element quantifies its importance in the process. The greater the value of SS, the greater the importance of the associated element in the process.

Analysis of variance (ANOVA) tests showed that the initial concentration C_i of CV dye was considered the most significant factor of adsorption efficiency with a percentage contribution of 51.56 %. The contact time t_c (29.18 %) and the bioadsorbent ratio (18.76 %) have a moderate influence on the adsorption, whereas the effects of pH (0.27 %) and temperature T (0.16 %) are negligible. On the other hand, for Orange G, the bioadsorbent ratio is the main factor for the adsorption efficiency with a percentage contribution of (56.41 %). Furthermore, the percentage contribution of the contact time t_c (24 %) together with the initial concentration C_i (13.88 %) is moderate, while the pH (4.36 %) is a factor to be taken into account and the temperature T (0.27 %) is negligible.

In addition, we find that the confidence level of these tests for CV and OG dyes is 99.93 % and 98.92 % as well as the margin of error is only 0.07 % and 1.08 %, respectively. The relative importance of the different factors is also reflected in the following figure (Fig. 4).

3.2.3. Graphical representation of the impacts and interactions of the main parameters

3.2.3.1. Plotting the average impacts. The average effects of a parameters are determined by the variation in response found as the parameter varies from one modality to another. The representation of the impacts by a line segment makes it possible to identify their sign and their amplitude. The effects of the tested parameters on the percentage of dye elimination by TPCE can be seen in (Fig. 5a and b).

3.2.3.2. The impact of the initial dye concentration. For both systems, the initial dye concentration is an essential factor in the adsorption mechanism. The influence of the initial dye concentration was investigated in the range of 20–200 mg/L. As the concentration increases, the active sites on the surface of the bioadsorbent are quickly saturated by the dye molecules. Therefore, the percentage of adsorption is reduced. We also found that the negative sign of the initial concentration for both systems means that pollutant removal is preferred at low concentration values.

3.2.3.3. The impact of the bioadsorbent ratio. The higher the amount of sorbent, the more free and unused sites exist on the biomaterial, implying the presence of a larger contact area for the dye molecules [59].

Table 3
TED for the five two-level parameters of the adsorbent/adsorbate system.

tests	Bioadsorbent ratio (g/L)	Contact time (min)	Initial Concentration (mg/L)	Temperature (C°)	pH	Removal %	
						CV	OG
1	3	5	20	18	4	95.64	40.35
2	3	5	20	35	10	97.93	38.77
3	3	60	200	18	4	64.64	49.76
4	3	60	200	35	10	66.87	38.75
5	15	5	200	18	10	89.44	47.75
6	15	5	200	35	4	90.08	61.66
7	15	60	20	18	10	94.76	85.76
8	15	60	20	35	4	93.53	92.68

From these results, it can be seen that the optimal elimination of CV dye by the adsorbent was 97.93 % under the following optimal parameters: R = 3 g/L, pH 10, C_i = 20 mg/L, T = 35 °C, and t_c = 5 min. While the minimum removal of 20.87 % was achieved for R = 3 g/L, pH 4, C_i = 200 mg/L, T = 18C°, and t_c = 60 min. For OG, the maximum elimination was achieved at 92.68 % at the following optimal values: R = 15 g/L, pH 4, T = 35C°, C_i = 20 mg/L, with t_c = 60 min. On the other hand, the minimum orange G elimination of 38.75 % at R = 3 g/L, pH 10, T = 35C°, C_i = 200 mg/L and t_c = 60 min.

Table 4
ANOVA results on adsorption efficiency.

Source of variance	Degree of freedom		Sum of squares (SS)		Contribution	
	CV	OG	CV	OG	CV	OG
Bioadsorbent ratio (g/L)	1		228.23	1806.61	18.76 %	**56.41 %**[a]
Contact time (min)	1		354.98	768.71	29.18 %	24.00 %
Initial Concentration (mg/L)	1		627.11	444.62	**51.56 %**[a]	13.88 %
Temperature (°C)	1		1.93	8.49	0.16 %	0.27 %
pH	1		3.26	139.61	0.27 %	4.36 %
Error	2		0.88	34.45	0.07 %	1.08 %
Total	7		1216.39	3202.48	100.00 %	100.00 %

[a] The most important factor.

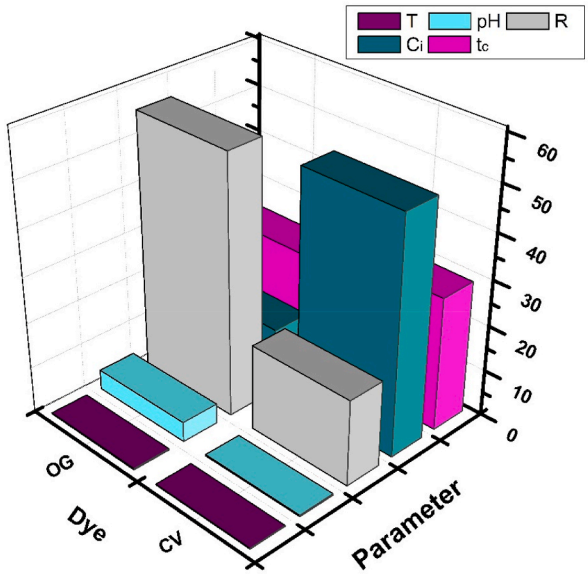

Fig. 4. Factors of influence on the adsorption process of CV and OG dyes on TPCE.

The positive sign of the ratio for the TPCE/OG and TPCE/CV systems means that dye removal was favored at high f adsorbent values. Increasing the TPCE mass from 0.1 to 0.6 g increased the percentage of adsorption; this is caused by the increase in active or surface sites for a large amount of biomaterial. The influence of the ratio on the percentage is not proportional for both systems studied, which is consistent with the argument of the nature of the dyes and the surface sites of the adsorbent.

3.2.3.4. The impact of the contact time. To achieve the equilibrium between the aqueous solution and the biomaterial, the time factor is important and mainly affects the adsorption percentage. Consequently, the adsorption time was studied in the interval of 5–60 min.

The positive sign of time for the TPCE/OG system as the contact time increases to 60 min means that dye removal was favored at high contact time values. In contrast, increasing the contact time from 5 to 60 min for TPCE/CV decreased the percentage of adsorption.

The difference in kinetic performance and sign of the tested adsorbed/adsorbent systems is due to the nature of the dyes and biomaterial. The rapidity of adsorption for the TPCE/CV system is mainly explained by the fact that CV contains one cationic $C{=}N^{+}$ site while OG has two anionic $C–SO^{3-}$ (sulfonate) sites, as well as the difference in molecular size of these dyes. The fact that the contact time of CV is shorter than the contact time of OG suggests that the studied bioadsorbent surface contains more anionic than cationic adsorption sites. In addition, OG is bulky, has a higher molecular weight and a greater surface area (length) than CV.

3.2.3.5. The impact of the pH. We note that for TPCE, the pH_z value is in the range of 7. The bioadsorbent particles' surfaces become negatively charged for pH values above pH_z, which facilitates the adsorption of cationic substances like CV, which has a cationic nitrogen site. They become positively charged at lower pH levels and are attracted to anionic dyes like OG [60].

The positive sign of pH for the TPCE/CV system means that dye removal was favored at higher pH values. Due to the increase in pH and the alkaline nature of the solution, the surface of the bioadsorbent becomes increasingly negative, which enhances the phenomenon of electrostatic interactions between the biomaterial and the dye, which is consistent with the observed value of CV adsorption, as shown in Fig. 5 a. Orange G is an anionic dye with two sulfonate anions in each molecule. The adsorption of this dye in

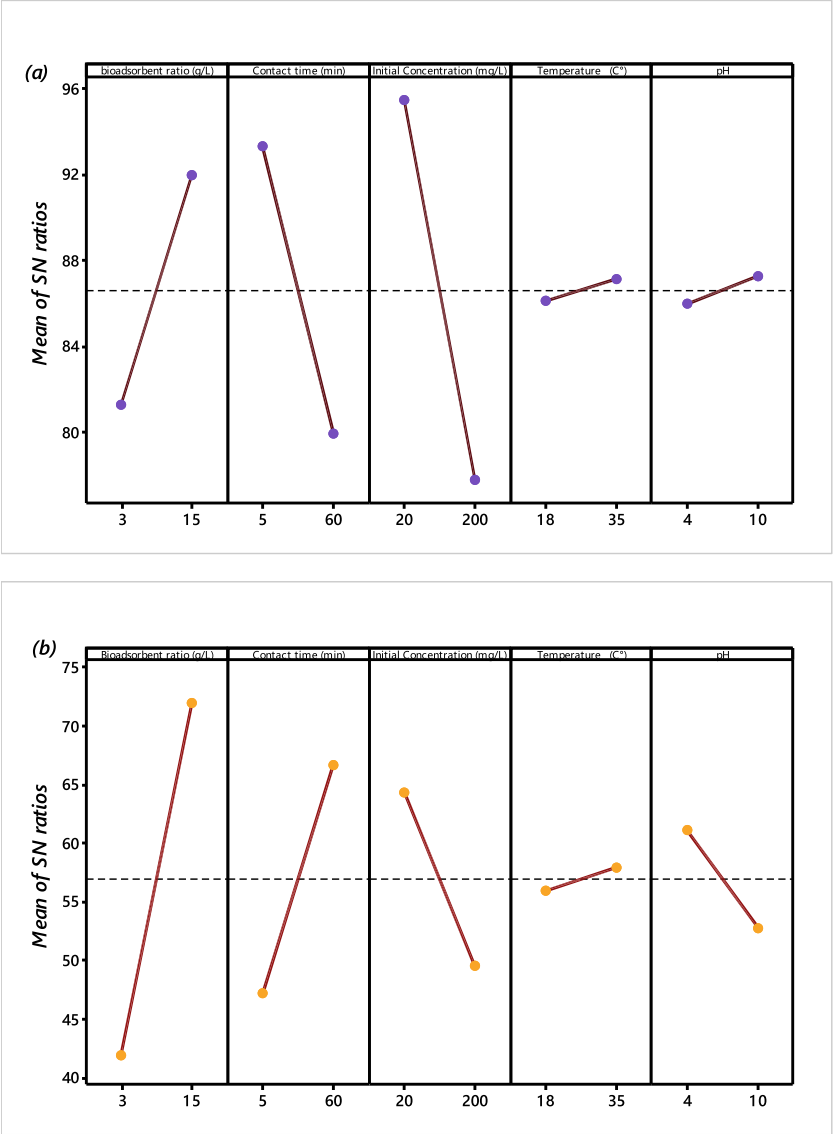

Fig. 5. Impacts of the main parameters on the percentage of dye adsorption: (a) CV, (b) OG.

the base medium is limited by the repulsive forces present between the negatively charged dye molecule groups and the negatively charged biomaterial sites. We can see that the negative sign of the percent elimination is inversely proportional to the pH, which means that good elimination is inversely proportional to the pH, which means that good elimination efficiency is achieved for the most acidic pH (pH = 4) for the TPCE/OG system.

3.2.3.6. The impact of the temperature. The influence of temperature plays a significant role in the adsorption system because a temperature fluctuation can vary the equilibrium constant and the adsorption amount of the biomaterial for a particular solute. The positive sign of temperature for both TPCE/OG and TPCE/CV systems means that dye removal is favored at higher temperature values. We also find that the percentage removal of crystal violet and orange G on the TPCE support increases slightly with increasing temperature from 18 to 35 °C. This indicates that the adsorption process is endothermic, which may be related to the increase in mobility of molecules with increasing temperature [61]. This could be explained by the homogeneity of the surface of the TPCE biomaterial demonstrated by SEM.

3.2.4. Interactions between the main factors governing adsorption

In a complex system, the parameters are often coupled, and the variation of one factor can influence the other factors.

The interactions between the different factors (at levels −1 and +1) affecting the adsorption of CV and OG dyes on the used biomaterial are shown in (Fig. 6a and b).

The diagram shows the interactions between the different parameters at both high and low levels (−1 and +1). An interaction is expressed by the fact that the two lines are not parallel. The more the lines deviate from parallelism, the higher the degree of interaction. From the diagram we can see that the most important interactions concern the following combinations.

- Initial concentration - bioadsorbent ratio,
- Initial concentration - contact time,
- Bioadsorbent ratio - contact time.

On the other hand, the other interactions are weak because the lines of the corresponding plot are almost parallel.

3.2.5. *Modeling of the adsorption process by linear regression*

Modeling and prediction of an equation related to the adsorption process of CV and OG dye on TPCE biomaterial was carried out using linear regression analysis [62].

The correlation coefficients (R^2) were 0.9993 and 0.9892, and the adj-R^2 were 0.9975 and 0.9624 for CV and OG, respectively. The high R^2 and adj-R^2 values enhance the model's ability to provide a satisfactory assessment of the response. The theoretical prediction equations obtained by the linear regression model related to the adsorption performance as a function of the studied control factors are

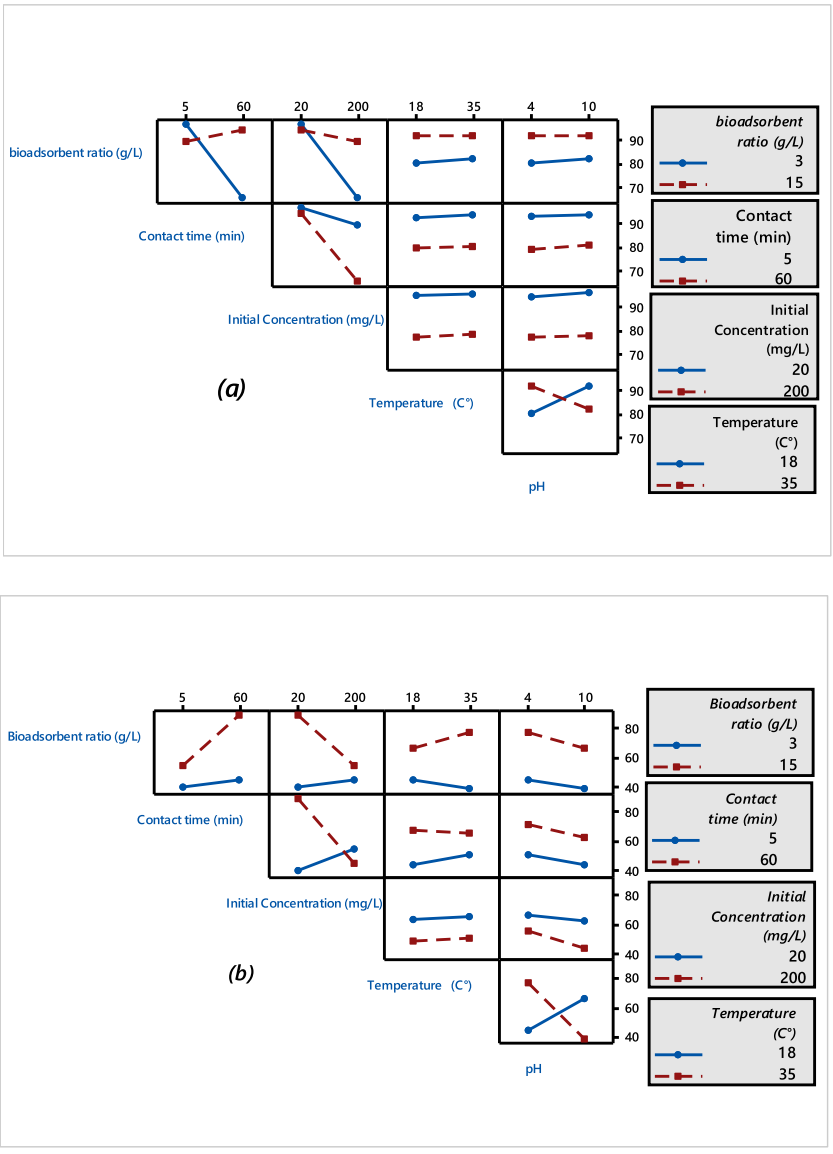

Fig. 6. Interactions of the main factors on adsorption at the TPCE/dye interface: (a) CV, (b) OG.

given in Equations (2) and (3) below.

$$R\%\_CV = 94.27 + 0.8902\,R - 0.24223t_c - 0.09837C_i + 0.0578\,T + 0.2129\,pH \quad (2)$$

$$R\%\_OG = 38.46 + 2.505\,R + 0.3565t_c - 0.0828C_i + 0.121\,T - 1.392\,pH \quad (3)$$

with R: bioadsorbent ratio; t_c: contact time; C_i: initial concentration; T: temperature.

The experimental values of the response R are compared with the values of R calculated by the applied model and their difference is called the residual. These residuals are used to test the quality of the model. To compare our experimental tests with the theoretical values, we correlated the values predicted by the model with the values measured during the experimental tests (Fig. 7a and b). From this figure, we can see that the results of the real tests (points) are aligned with the line y = x, which corresponds to the values predicted by the theoretical model, indicating that the obtained values are normal and symmetrical. This proves that there are no anomalous or outlier values.

We can therefore say that the obtained theoretical prediction equations well describe the adsorption process studied for the TPCE/CV and TPCE/OG system. The experimental results confirm that the established equations represent a good relationship between the parameters and the response, and the confidence level of this test is 99.93 % and 98.92 % for CV and OG, respectively.

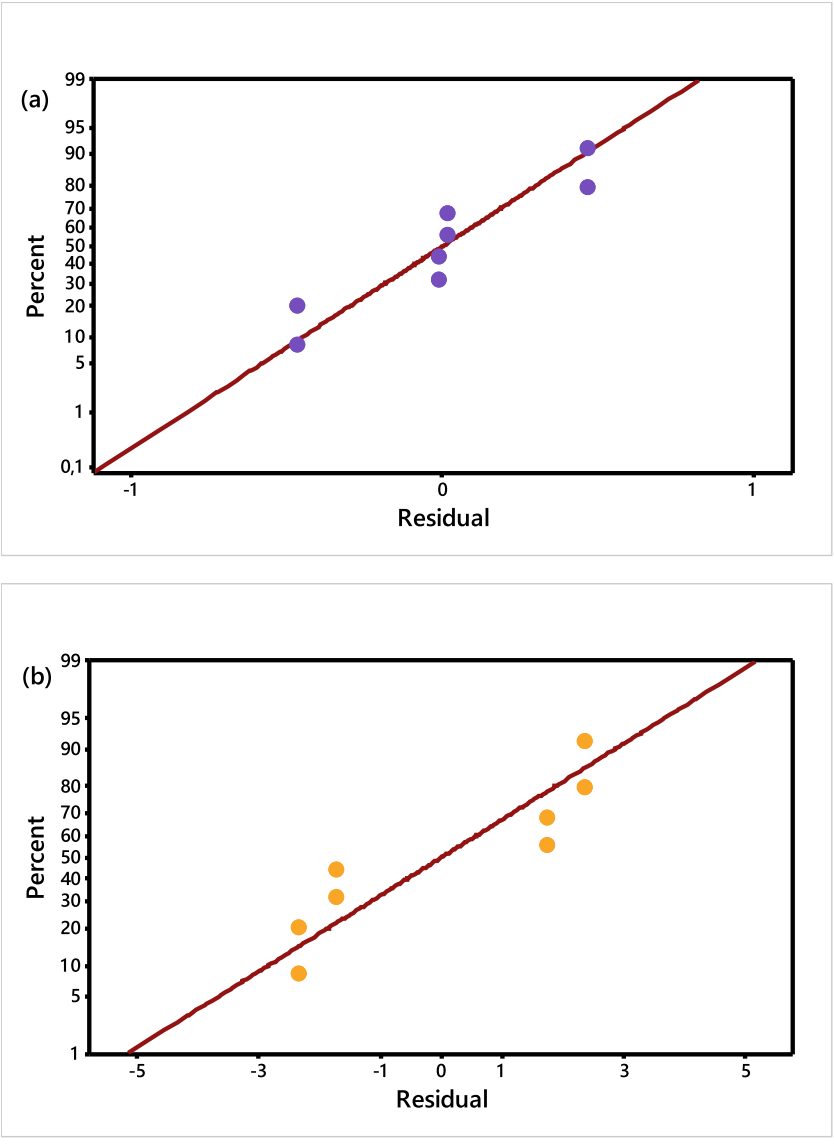

Fig. 7. Graphical representations of predicted values Vs experimental values: (a) CV, (b) OG.

3.2.6. Significant variable optimization by RSM

After studying the parameters affecting the elimination of CV and OG dyes using the Taguchi approach, the factors for dye elimination from solution were improved using RSM. Based on the tests conducted in the Taguchi plan, the initial dye concentrations, bioadsorption ratio and contact time are the significant factors affecting the elimination of CV and OG dyes in the process. These elements were considered the most significant parameters (independent variables) in the Box-Behenken model of the Surface Response Methodology (RSM).

The results for the CV and OG dyes are shown in Table 5. The correlation coefficients (R^2) were 0.9999 and 0.9999, and adj-R^2 were 0.9997 and 0.9999 for the CV and OG dyes, respectively. The good values of R^2 and adj-R^2 strengthen the model's ability to perform reliable response estimation. As shown in Table 5, the p-value for the linear parameters and the interaction parameters is less than 0.05. From the p-value associated with the nonconformity, it can be concluded that the derived equation agrees with the experimental results.

Fig. 8 shows the three-dimensional diagrams of the interaction effects. Three-dimensional surface response plots are a relationship of two independent factors that keep the other factor at a constant level. These charts can provide insight into the relationship between the two factors and are helpful in understanding the main and interrelationships of the two factors.

Fig. 8a,A demonstrates the interaction of the two factors adsorbent ratio and contact time in the elimination of the two dyes. Dye elimination increases with increasing contact time and adsorbent ratio. With increasing contact time, adsorption increases due to the presence of free active sites on the biomaterial surface. In addition, increasing the adsorbent ratio provides more adsorption sites for the adsorption of the dye molecules on the surface of the biomaterial. Consequently, the interaction of these two factors, leading to a positive biomaterial surface area and more adsorption sites, increases adsorption. According to Fig. 8b,B, the percentage of dye removed decreases as the dye concentration of CV and OG increases. The reduction in percent elimination at higher concentrations is caused by the increase in dye concentration as a function of the number of initial dye molecules present on the surface. For a given adsorbent ratio, the total number of active sites available is constant and therefore the same amount of sites absorb the analyte, so as the initial dye concentration increases, the percent elimination decreases. Fig. 8c,C shows the effect of initial dye concentration and contact time on the percentage of dye removed. It is known that as the contact time increases, the percentage of dye removed must increase. Because the longer the time, the greater the chance that the dye and adsorption molecules will be exposed.

3.3. DFTB+

The optimized geometry for studying the adsorption interaction between the adsorbent and the CV or OG is shown in (Fig. 9a and b).

The interaction energy between the OG and CV dyes and the adsorbents strongly depends on the molecular geometry and the intrinsic electronic properties during adsorption [40]. The configuration and orientation of the adsorbate molecules on the surface of the adsorbents, as well as the electronic properties of the molecules themselves, have a significant influence on the efficiency of the interaction [47,63]. These parameters play an essential role in determining the strength and nature of the interaction between adsorbate and adsorbent and thus influence the entire adsorption process [37,44,52,64].

3.4. Monte Carlo MD simulations

Recognizing the ideal adsorption arrangement of the adsorbate on the adsorbent is fundamental to calculating surface affinity. The

Table 5
Analysis of variance for the quadratic polynomial model for elimination of CV and OG. A: Adsorbent ratio (g/L), B: Contact time (min), C: Initial Concentration (mg/L).

		CV				*OG*			
Source	DF	Sum of Squares	Mean Square	F-value	p-value	Sum of Squares	Mean Square	F-value	p-value
Model	9	203.12	22.57	4817.16	<0.0001	5063.64	562.63	3.553E+06	<0.0001
A-A	1	72.78	72.78	15535.14	<0.0001	2264.31	2264.31	1.430E+07	<0.0001
B–B	1	9.33	9.33	1991.72	<0.0001	1188.53	1188.53	7.506E+06	<0.0001
C–C	1	68.50	68.50	14621.88	<0.0001	506.57	506.57	3.199E+06	<0.0001
AB	1	1.54	1.54	328.20	<0.0001	120.34	120.34	7.600E+05	<0.0001
AC	1	4.95	4.95	1056.70	<0.0001	22.42	22.42	1.416E+05	<0.0001
BC	1	0.1444	0.1444	30.82	0,0026	10.02	10.02	63266.68	<0.0001
A^2	1	33.81	33.81	7217.68	<0.0001	695.71	695.71	4.394E+06	<0.0001
B^2	1	14.09	14.09	3008.34	<0.0001	225.31	225.31	1.423E+06	<0.0001
C^2	1	2.90	2.90	619.01	<0.0001	148.61	148.61	9.386E+05	<0.0001
Residual	5	0.0234	0.0047			0.0008	0.0002		
Lack of Fit	3	0.0234	0.0078			0.0005	0.0002	1.31	0.4600
Pure Error	2	0.0000	0.0000			0.0003	0.0001		
Cor Total	14	203.14				5063.64			
Model summary statistics		***CV***				***OG***			
		R^2	Adj-R^2	Pred-R^2		R^2	Adj-R^2	Pred-R^2	
		0.9999	0.9997	0.9982		0.9999	0.9999	0.9999	

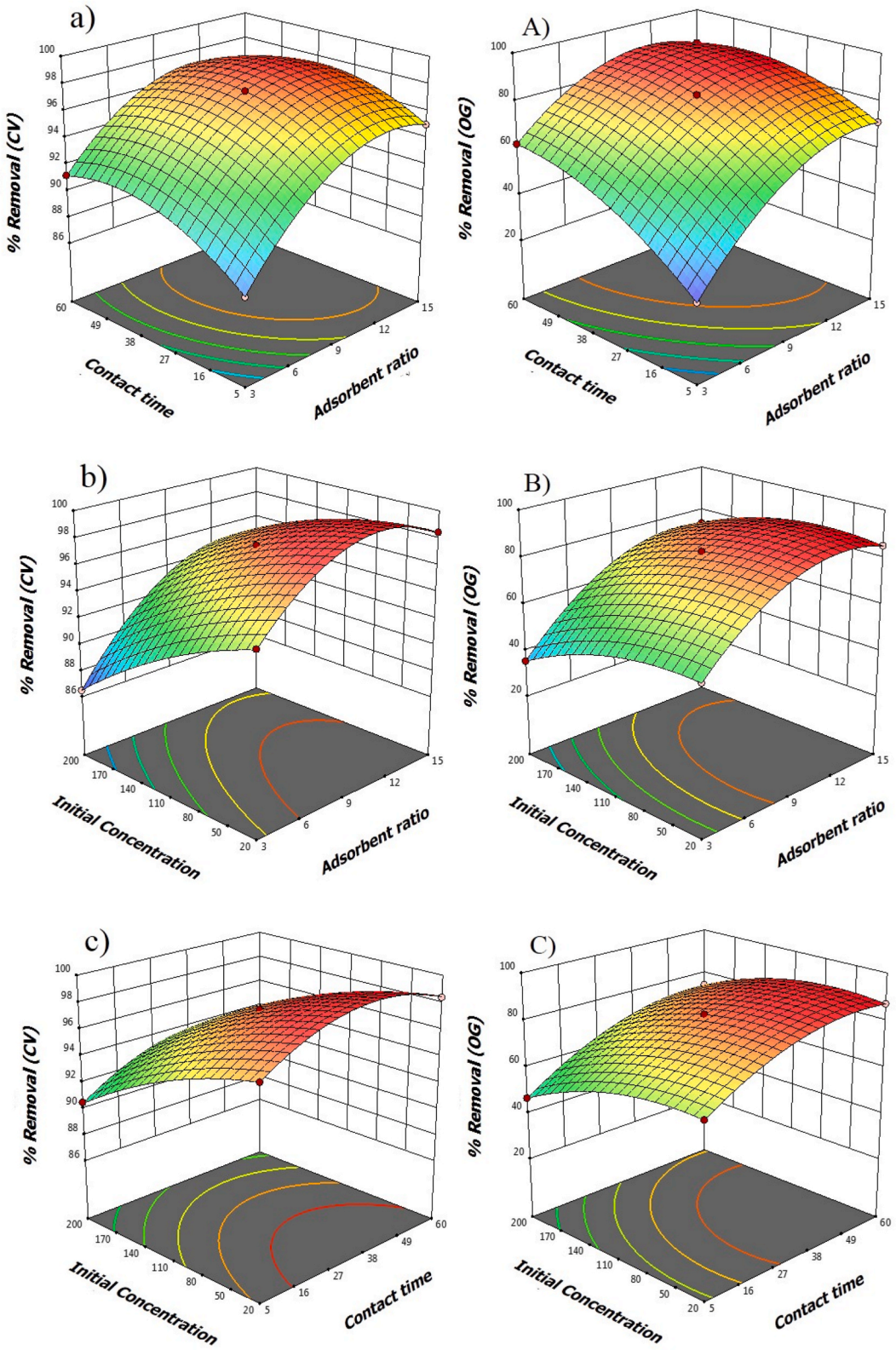

Fig. 8. Response surface graphs of elimination of (a,b,c) CV and (A,B,C) OG.

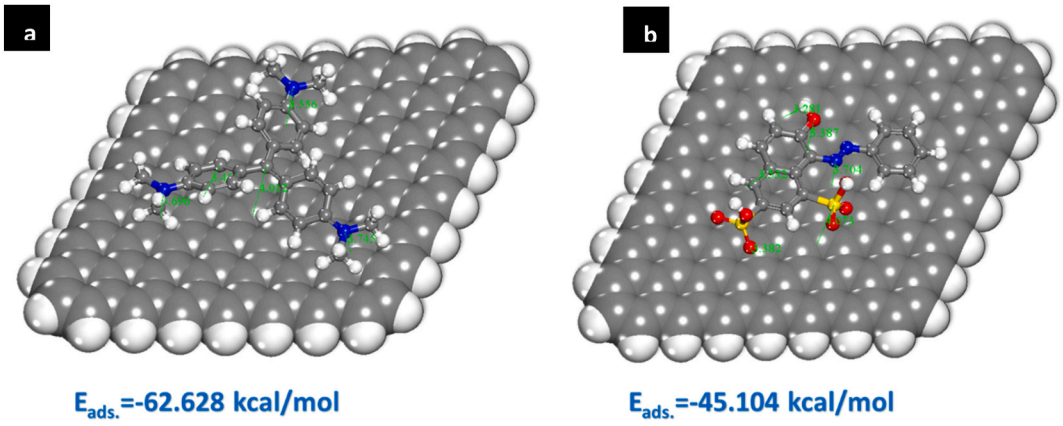

Fig. 9. The lowest energy adsorption poses for the dye as obtained via DFTB + calculations: (a) CV, (b) OG.

adsorption energy (E_{ads}) calculation of this approach is based on the interaction of the adsorbate with the adsorbent. This is often achieved quantitatively by determining adsorption using the following equation (4) [48,65–68]:

$$E_{adsorption} = E_{Adsorbent/Adsorbate} - (E_{adsorbent} + E_{adsorbate}) \quad (4)$$

where $E_{Adsorbent/adsorbate}$ is the total energy of the simulated adsorption system, $E_{adsorbate}$ and $E_{adsorbent}$ are the total energies of the adsorbate molecules (CV or OG) and the adsorbent.

This method of assessing molecular complexity depends on generating an enormous variety of combinations of the species (molecules, ions) used in the simulation. These combinations are randomly generated [38,41,44,51,52,56,69]. The adsorption geometries of the adsorbate molecules are shown in Fig. 10.

The results of the experiment are confirmed by the fact that a significantly higher negative value of E_{ads} was observed when the adsorbate molecules were loaded onto the adsorbent surface (Fig. 11) [40,43,45,47].

In general, MD simulations are used to analyze and understand how molecules behave and interact with material surfaces [43,46,67,68]. These simulations provide a computational framework for investigating adsorption dynamics. Fig. 12 shows the final configuration of the adsorbate molecules on the surface of the adsorbent after MD simulation [38,48,51]. To investigate the behavior of atoms and molecules over time, MD simulations use a number of computational processes. The first step is to establish the system by placing adsorbate molecules on the surface of the material (in this case the geometry obtained via MC).

To ensure that the system components possess the least amount of energy feasible, one technique involves monitoring and controlling temperature fluctuations during MD simulation [42,48,68]. This method attempts to minimize any temperature fluctuations that may occur.

Fig. 12 shows that the temperature fluctuations observed during MD simulation are negligible, supporting the effectiveness of this method. This indicates that the MD simulation of our system succeeded in maintaining a stable and well-regulated energy state. In addition, the Radial Distribution Function (RDF) analysis technique is used to study the MD trajectory obtained from adsorption experiments (as shown in Fig. 13). RDF analysis provides a simple method for interpreting the underlying physisorption or chemisorption processes that occur during adsorption on the surface of the material [44–46,64,68]. By examining the RDF, researchers can gain insights into the spatial distribution and arrangement of adsorbate molecules relative to the adsorbent surface, thereby improving their understanding of the adsorption phenomenon. This analysis helps distinguish between physical interactions (physisorption) and chemical bonds (chemisorption) that occur during the adsorption process.

The presence of peaks in the RDF diagram at certain distances from the material surface indicates the nature of the adsorption process [38,43,44,46,51]. If the peak is observed between 1 and 3.5 Å, it suggests the involvement of a chemisorption process [65,70]. However, if the RDF peaks are at distances of more than 3.5 Å, this indicates the occurrence of a physisorption process [38,45,51,64,67,71]. In this scenario, when the RDF peak is between 1 and 3.5 Å, it indicates the likelihood of a chemisorption process. Conversely, if the RDF peaks are observed at distances greater than 3.5 Å, this indicates the presence of a physisorption process. Notably, RDF analysis indicates that nitrogen (N) is not involved in the adsorption process, while oxygen (O) peaks near the boundary between chemisorption and physisorption. Examining the example of the dye molecules, it becomes clear that they interact strongly with the adsorbent surface [42,43,51]. This is supported by their significantly negative adsorption energy value and the presence of distinct RDF peaks, confirming their substantial interaction and binding with the adsorbent surface [38,51].

3.5. Desorption and reuse study

The reusability of bioadsorbent represents one of the most important economic criteria. For this reason, the reusability of the TPCE biomaterial was investigated during the CV and OG adsorption phenomenon and reapplied under optimal conditions. During this work, the TPCE used was rinsed for a defined time with 20 mL of nitric acid solution (0.1 N) for CV and sodium hydroxide solution (0.5

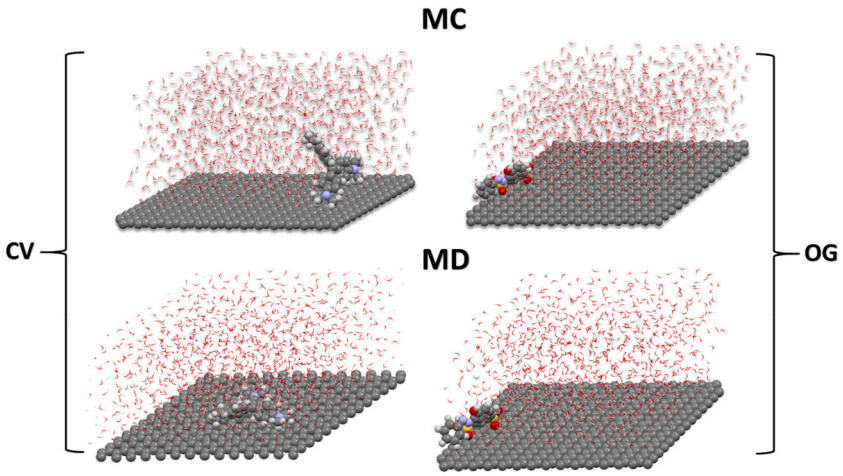

Fig. 10. The lowest energy adsorption poses for the CV and OG as obtained via MC and MD calculations.

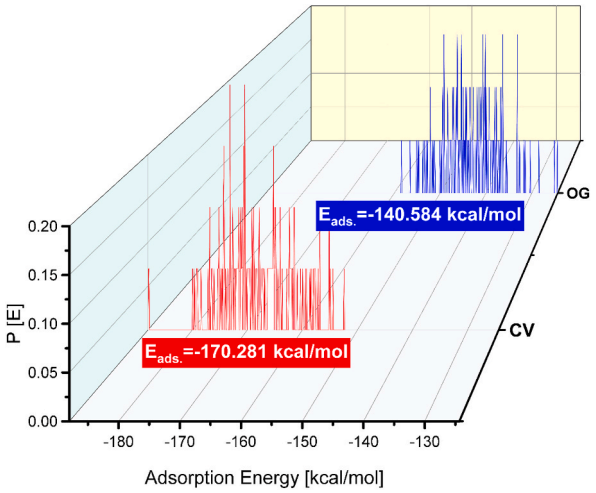

Fig. 11. Distribution of the adsorption energies as obtained from MC calculation.

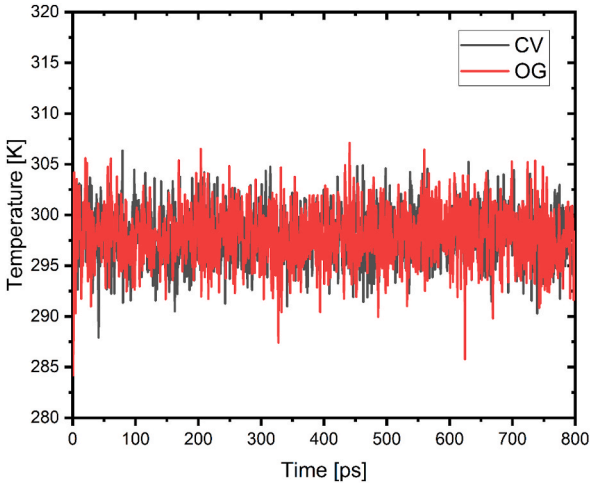

Fig. 12. Temperature fluctuations during MD simulation of the dye adsorption process.

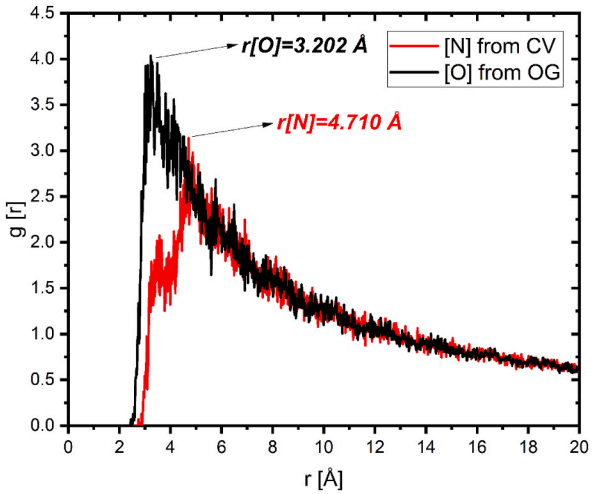

Fig. 13. RDF of heteroatoms (O and N) for the CV and OG dyes onto the adsorbent surface obtained via MD.

N) for OG. As a final step, the adsorption capacity for each run was determined spectrophotometrically. The data in Fig. 14 shows that the adsorption performance decreases slightly after five cycles. Overall, the percent removal of CV and OG dye were found to be 97.93 % and 92.68 %, and then decreased to 86.42 % and 78.84 %, respectively after five uses. This decrease is probably attributable to the degradation of adsorption during adsorption-desorption cycles [72].

4. Conclusion

The performance of TPCE biomaterial in the simultaneous elimination of crystal violet (CV) and orange G (OG) dyes from aqueous solutions was investigated. The prepared biosorbent was analyzed by SEM-EDX, FT-IR, pH_z, and (Ss). The main factors affecting the dye elimination process were identified using the Taguchi approach. These useful parameters, namely solution pH, bioadsorbent ratio, contact time, temperature, and dye concentrations were optimized using TED and RSM methods. The optimal parameters determined using TED modeling were as follows 3 g/L, pH 10, 20 mg/L, 35 °C, 5 min and 15 g/L, pH 4, 20 mg/L, 35 °C, 60 min for CV and OG dyes, respectively. Maximum dye elimination (over 92 %) was observed for each dye. Linear models for both dye identifications were statistically fit with $R^2 > 0.98$ values and the data indicated that both models have good precision. The data from the adsorption-desorption tests indicated that the bioadsorbent can be reused for up to five cycles without a noticeable decrease in the percentage dye elimination. The Density Functional Tight Binding (DFTB) method shows that dyes strongly bind the adsorbent surface. Monte Carlo and Molecular Dynamics simulations show significant interactions between dye and adsorbent surface. These simulations provide information about the molecular dynamics of the dye during adsorption. These computational conclusions are consistent with experimental data and confirm the accuracy and reliability of the simulation. These discoveries can improve experimental design by developing better methods to remove dyes from the environment using the prepared adsorbent material. In addition, they can provide a theoretical basis for adsorption, explaining the mechanisms and interactions of dye adsorption. These results are useful for

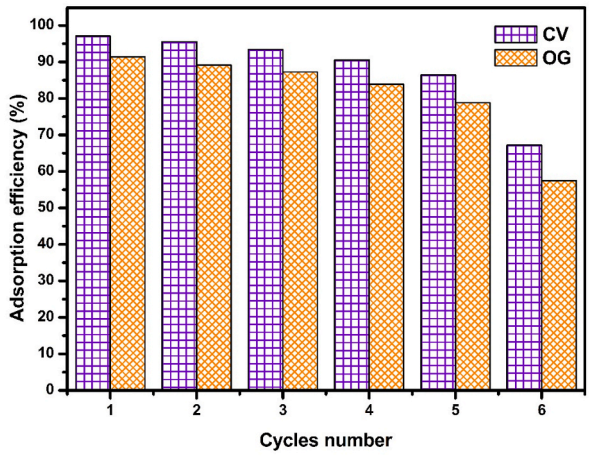

Fig. 14. Impact of the number of regeneration cycles on dye adsorption on TPCE biomaterial.

developing new materials and methods for environmental remediation or dye removal.

Funding

The authors declare that no funds, grants, or other support were received during the preparation of this manuscript.

Ethical approval

Not applicable.

Consent to participate

Not applicable.

Consent to publish

Not applicable.

Data availability statement

Data will be made available on request.

CRediT authorship contribution statement

Abdelkader Dabagh: Writing – original draft, Methodology, Investigation, Funding acquisition, Formal analysis. **Ridouan Benhiti:** Writing – original draft, Methodology, Formal analysis. **Mohamed EL-Habacha:** Writing – original draft, Methodology, Formal analysis. **Abdeljalil Ait Ichou:** Writing – review & editing, Investigation. **M'hamed Abali:** Writing – review & editing, Investigation. **Abdallah Assouani:** Writing – review & editing, Investigation. **Mahmoudy Guellaa:** Writing – review & editing, Investigation. **Avni Berisha:** Writing – review & editing. **Rachid Hsissou:** Writing – review & editing, Investigation. **Fouad Sinan:** Writing – review & editing, Supervision, Methodology. **Mohamed Zerbet:** Writing – review & editing, Supervision.

Declaration of competing interest

The authors declare that they have no known competing financial interests or personal relationships that could have appeared to influence the work reported in this paper.

References

[1] M. Sarabadan, H. Bashiri, S.M. Mousavi, Removal of crystal violet dye by an efficient and low cost adsorbent: modeling, kinetic, equilibrium and thermodynamic studies, Kor. J. Chem. Eng. 36 (2019) 1575–1586.
[2] P. Naderi, M. Shirani, A. Semnani, A. Goli, Efficient removal of crystal violet from aqueous solutions with Centaurea stem as a novel biodegradable bioadsorbent using response surface methodology and simulated annealing: kinetic, isotherm and thermodynamic studies, Ecotoxicol. Environ. Saf. 163 (2018) 372–381, https://doi.org/10.1016/j.ecoenv.2018.07.091.
[3] G.K. Sarma, S. Sen Gupta, K.G. Bhattacharyya, Removal of hazardous basic dyes from aqueous solution by adsorption onto kaolinite and acid-treated kaolinite: kinetics, isotherm and mechanistic study, SN Appl. Sci. 1 (2019) 1–15.
[4] H.A. Al-Yousef, B.M. Alotaibi, M.M. Alanazi, F. Aouaini, L. Sellaoui, A. Bonilla-Petriciolet, Theoretical assessment of the adsorption mechanism of ibuprofen, ampicillin, orange G and malachite green on a biomass functionalized with plasma, J. Environ. Chem. Eng. 9 (2021), 104950.
[5] A. Rana, K. Qanungo, Orange G dye removal from aqueous-solution using various adsorbents: A mini review, Mater Today Proc 81 (2021) 754–757.
[6] B. Dash, A. Kumar, Nanofiltration for textile dye–water treatment: experimental and parameter estimation studies using a spiral wound module and validation of the Spiegler–Kedem-based model, Sep Sci Technol 52 (2017) 1216–1224.
[7] G. Han, C.-Z. Liang, T.-S. Chung, M. Weber, C. Staudt, C. Maletzko, Combination of forward osmosis (FO) process with coagulation/flocculation (CF) for potential treatment of textile wastewater, Water Res. 91 (2016) 361–370.
[8] I. Anastopoulos, M. Karamesouti, A.C. Mitropoulos, G.Z. Kyzas, A review for coffee adsorbents, J. Mol. Liq. 229 (2017) 555–565.
[9] F.C. Moreira, R.A. Boaventura, E. Brillas, V.J. Vilar, Electrochemical advanced oxidation processes: a review on their application to synthetic and real wastewaters, Appl. Catal. B Environ. 202 (2017) 217–261.
[10] B.H. Fard, R.R. Khojasteh, P. Gharbani, Preparation and characterization of Visible-light sensitive nano Ag/Ag3VO4/agVO3 modified by graphene oxide for photodegradation of reactive orange 16 dye, J. Inorg. Organomet. Polym. Mater. 28 (2018) 1149–1157, https://doi.org/10.1007/s10904-018-0798-7.
[11] D. Huang, C. Hu, G. Zeng, M. Cheng, P. Xu, X. Gong, et al., Combination of Fenton processes and biotreatment for wastewater treatment and soil remediation, Sci. Total Environ. 574 (2017) 1599–1610.
[12] P. Liang, M. Rivallin, S. Cerneaux, S. Lacour, E. Petit, M. Cretin, Coupling cathodic Electro-Fenton reaction to membrane filtration for AO7 dye degradation: a successful feasibility study, J. Membr. Sci. 510 (2016) 182–190.
[13] G.P. Singaravel, R. Hashaikeh, Fabrication of electrospun LTL zeolite fibers and their application for dye removal, J. Mater. Sci. 51 (2016) 1133–1141.
[14] K. Zare, V.K. Gupta, O. Moradi, A.S.H. Makhlouf, M. Sillanpää, M.N. Nadagouda, et al., A comparative study on the basis of adsorption capacity between CNTs and activated carbon as adsorbents for removal of noxious synthetic dyes: a review, J Nanostructure Chem 5 (2015) 227–236.
[15] I. Salehi, M. Shirani, A. Semnani, M. Hassani, S. Habibollahi, Comparative study between response surface methodology and artificial neural network for adsorption of crystal violet on magnetic activated carbon, Arabian J. Sci. Eng. 41 (2016) 2611–2621, https://doi.org/10.1007/s13369-016-2109-3.
[16] M. Shahrashoub, S. Bakhtiari, The efficiency of activated carbon/magnetite nanoparticles composites in copper removal: industrial waste recovery, green synthesis, characterization, and adsorption-desorption studies, Microporous Mesoporous Mater. 311 (2021), 110692.

[17] N. El Messaoudi, M. El Khomri, A. Dabagh, Z.G. Chegini, A. Dbik, S. Bentahar, et al., Synthesis of a novel nanocomposite based on date stones/CuFe2O4 nanoparticles for eliminating cationic and anionic dyes from aqueous solution, Int. J. Environ. Stud. 79 (2022) 417–435.

[18] T.B. Vidovix, H.B. Quesada, R. Bergamasco, M.F. Vieira, A.M.S. Vieira, Adsorption of Safranin-O dye by copper oxide nanoparticles synthesized from Punica granatum leaf extract, Environ. Technol. 43 (2022) 3047–3063.

[19] M. Zahedifar, M. Shirani, A. Akbari, N. Seyedi, Green synthesis of Ag2S nanoparticles on cellulose/Fe3O4 nanocomposite template for catalytic degradation of organic dyes, Cellulose 26 (2019) 6797–6812, https://doi.org/10.1007/s10570-019-02550-6.

[20] A. Ghazali, M. Shirani, A. Semnani, V. Zare-Shahabadi, M. Nekoeinia, Optimization of crystal violet adsorption onto Date palm leaves as a potent biosorbent from aqueous solutions using response surface methodology and ant colony, J. Environ. Chem. Eng. 6 (2018) 3942–3950.

[21] S. Dey, P. Bhagat, J. Mohanta, B. Dey, Methylene blue removal using eucalyptus leaves: a low cost protocol towards environmental sustainability, Eur J Adv Chem Res 3 (2022) 1–11.

[22] D.T.C. Nguyen, T.V. Tran, P.S. Kumar, A.T.M. Din, A.A. Jalil, D.-V.N. Vo, Invasive plants as biosorbents for environmental remediation: a review, Environ. Chem. Lett. 20 (2022) 1421–1451.

[23] A. Dabagh, A. Bagui, M. Abali, R. Aziam, M. Chiban, F. Sinan, et al., Adsorption of Crystal Violet from aqueous solution onto eco-friendly native Carpobrotus edulis plant, Mater Today Proc 37 (2021) 3980–3986.

[24] M. Abali, A. Ait Ichou, A. Zaghloul, M. Chiban, F. Sinan, M. Zerbet, Evaluation and improvement of the WWTP performance of an agricultural cooperative by adsorption on inert biomaterial: case of orthophosphate, nitrate and sulfate ions, Appl. Water Sci. 12 (2022) 1–9.

[25] G. Wang, S. Zhang, P. Yao, Y. Chen, X. Xu, T. Li, et al., Removal of Pb (II) from aqueous solutions by Phytolacca americana L. biomass as a low cost biosorbent, Arab. J. Chem. 11 (2018) 99–110.

[26] E.A. Dil, M. Ghaedi, A. Asfaram, The performance of nanorods material as adsorbent for removal of azo dyes and heavy metal ions: application of ultrasound wave, optimization and modeling, Ultrason. Sonochem. 34 (2017) 792–802.

[27] P. Gharbani, Modeling and optimization of reactive yellow 145 dye removal process onto synthesized MnOX-CeO2 using response surface methodology, Colloids Surf. A Physicochem. Eng. Asp. 548 (2018) 191–197, https://doi.org/10.1016/j.colsurfa.2018.03.046.

[28] E. Fathi, P. Gharbani, Modeling and optimization removal of reactive Orange 16 dye using MgO/g-C3N4/zeolite nanocomposite in coupling with LED and ultrasound by response surface methodology, Diam. Relat. Mater. 115 (2021), 108346, https://doi.org/10.1016/j.diamond.2021.108346.

[29] T. Kıvak, Optimization of surface roughness and flank wear using the Taguchi method in milling of Hadfield steel with PVD and CVD coated inserts, Measurement 50 (2014) 19–28, https://doi.org/10.1016/j.measurement.2013.12.017.

[30] S. Shojaei, S. Shojaei, S.S. Band, A.A.K. Farizhandi, M. Ghoroqi, A. Mosavi, Application of Taguchi method and response surface methodology into the removal of malachite green and auramine-O by NaX nanozeolites, Sci. Rep. 11 (2021), 16054, https://doi.org/10.1038/s41598-021-95649-5.

[31] F. Googerdchian, A. Moheb, R. Emadi, M. Asgari, Optimization of Pb(II) ions adsorption on nanohydroxyapatite adsorbents by applying Taguchi method, J. Hazard Mater. 349 (2018) 186–194, https://doi.org/10.1016/j.jhazmat.2018.01.056.

[32] N. Ramezani, F. Raji, M. Rezakazemi, M. Younas, Juglone extraction from walnut (Juglans regia L.) green husk by supercritical CO2: process optimization using Taguchi method, J. Environ. Chem. Eng. 8 (2020), 103776.

[33] W.-H. Chen, M.C. Uribe, E.E. Kwon, K.-Y.A. Lin, Y.-K. Park, L. Ding, et al., A comprehensive review of thermoelectric generation optimization by statistical approach: Taguchi method, analysis of variance (ANOVA), and response surface methodology (RSM), Renew. Sustain. Energy Rev. 169 (2022), 112917.

[34] A. Kumar, P.P. Srivastav, M. Pravitha, M. Hasan, S. Mangaraj, V. Prithviraj, et al., Comparative study on the optimization and characterization of soybean aqueous extract based composite film using response surface methodology (RSM) and artificial neural network (ANN), Food Packag. Shelf Life 31 (2022), 100778.

[35] B. Aradi, B. Hourahine, T. Frauenheim, DFTB+, a sparse matrix-based implementation of the DFTB method, J. Phys. Chem. A 111 (2007) 5678–5684, https://doi.org/10.1021/JP070186P.

[36] B. Hourahine, B. Aradi, V. Blum, F. Bonafé, A. Buccheri, C. Camacho, et al., DFTB+, a software package for efficient approximate density functional theory based atomistic simulations, J. Chem. Phys. 152 (2020), 124101, https://doi.org/10.1063/1.5143190.

[37] V. Mehmeti, M. Sadiku, A comprehensive DFT investigation of the adsorption of polycyclic aromatic hydrocarbons onto graphene, Computation 10 (2022) 68, https://doi.org/10.3390/computation10050068.

[38] R. Hamed, S. Jodeh, G. Hanbali, Z. Safi, A. Berisha, K. Xhaxhiu, et al., Eco-friendly synthesis and characterization of double-crossed link 3D graphene oxide functionalized with chitosan for adsorption of sulfamethazine from aqueous solution: experimental and DFT calculations, Front. Environ. Sci. 10 (2022) 977, https://doi.org/10.3389/fenvs.2022.930693.

[39] F. Spiegelman, N. Tarrat, J. Cuny, L. Dontot, E. Posenitskiy, C. Martí, et al., Density-functional tight-binding: basic concepts and applications to molecules and clusters 5 (2020), 1710252, https://doi.org/10.1080/23746149.2019.1710252.

[40] H. Babas, M. Khachani, I. Warad, S. Ajebli, A. Guessous, A. Guenbour, et al., Sofosbuvir adsorption onto activated carbon derived from argan shell residue: optimization, kinetic, thermodynamic and theoretical approaches, J. Mol. Liq. 356 (2022), 119019, https://doi.org/10.1016/j.molliq.2022.119019.

[41] A. Alija, D. Gashi, R. Plakaj, A. Omaj, V. Thaçi, A. Reka, et al., A theoretical and experimental study of the adsorptive removal of hexavalent chromium ions using graphene oxide as an adsorbent, Open Chem. 18 (2020) 936–942, https://doi.org/10.1515/chem-2020-0148.

[42] N. Nairat, O. Hamed, A. Berisha, S. Jodeh, M. Algarra, K. Azzaoui, et al., Cellulose polymers with β-amino ester pendant group: design, synthesis, molecular docking and application in adsorption of toxic metals from wastewater, BMC Chem 16 (2022) 1–21, https://doi.org/10.1186/s13065-022-00837-7.

[43] Ibrahim Abushqair, Avni Berisha, Dagdag Omar, Alaa Janem, Khalil Azzaoui, Rana Al-Kerm, B.H. Rola Al-Kerm, O.A. Hamed, M. Qaisi, I. Abushqair, A. Berisha, O. Dagdag, et al., Cellulose powder functionalized with phenyl biguanide: synthesis, cross-linking, metal adsorption, and molecular docking, Bioresources 16 (2021) 7263–7282, https://doi.org/10.15376/biores.16.4.7263-7282.

[44] N. Hasani, T. Selimi, A. Mele, V. Thaçi, J. Halili, A. Berisha, et al., Theoretical, equilibrium, kinetics and thermodynamic investigations of methylene blue adsorption onto lignite coal, Molecules 27 (2022) 1856, https://doi.org/10.3390/molecules27061856.

[45] V. Mehmeti, J. Halili, A. Berisha, Which is better for Lindane pesticide adsorption, graphene or graphene oxide? An experimental and DFT study, J. Mol. Liq. 347 (2022), 118345, https://doi.org/10.1016/j.molliq.2021.118345.

[46] O. Amrhar, A. Berisha, L. El Gana, H. Nassali, S. Elyoubi M, Removal of methylene blue dye by adsorption onto Natural Muscovite Clay: experimental, theoretical and computational investigation, Int. J. Environ. Anal. Chem. (2021) 1–26, https://doi.org/10.1080/03067319.2021.1897119.

[47] S. Ajebli, G. Kaichouh, M. Khachani, H. Babas, M. El Karbane, I. Warad, et al., The adsorption of Tenofovir in aqueous solution on activated carbon produced from maize cobs: insights from experimental, molecular dynamics simulation, and DFT calculations, Chem. Phys. Lett. 801 (2022), 139676, https://doi.org/10.1016/j.cplett.2022.139676.

[48] B. Khalaf, O. Hamed, S. Jodeh, R. Bol, G. Hanbali, Z. Safi, et al., Cellulose-based hectocycle nanopolymers: synthesis, molecular docking and adsorption of difenoconazole from aqueous medium, Int. J. Mol. Sci. 22 (2021), https://doi.org/10.3390/ijms22116090.

[49] R.L.C. Akkermans, N.A. Spenley, S.H. Robertson, COMPASS III: automated fitting workflows and extension to ionic liquids 47 (51) (2020) 540, https://doi.org/10.1080/08927022.2020.1808215.

[50] A. Berisha, F.I. Podvorica, R. Vataj, Corrosion inhibition study of mild steel in an aqueous hydrochloric acid solution using brilliant cresyl blue – a combined experimental and Monte Carlo study, Port. Electrochim. Acta 39 (2021) 393–401, https://doi.org/10.4152/pea.2021390601.

[51] O. Amrhar, H.-S. Lee, H. Lgaz, A. Berisha, E.E. Ebenso, Y. Cho, Computational insights into the adsorption mechanisms of anionic dyes on the rutile TiO2 (1 1 0) surface: combining SCC-DFT tight binding with quantum chemical and molecular dynamics simulations, J. Mol. Liq. 377 (2023), 121554, https://doi.org/10.1016/J.MOLLIQ.2023.121554.

[52] I. Lebkiri, B. Abbou, R. Hsissou, Z. Safi, M. Sadiku, A. Berisha, et al., Investigation of the anionic polyacrylamide as a potential adsorbent of crystal violet dye from aqueous solution: equilibrium, kinetic, thermodynamic, DFT, MC and MD approaches, J. Mol. Liq. 372 (2023), 121220, https://doi.org/10.1016/j.molliq.2023.121220.

[53] C. Tang, A. Farhadian, A. Berisha, M.A. Deyab, J. Chen, D. Iravani, et al., Novel biosurfactants for effective inhibition of gas hydrate agglomeration and corrosion in offshore oil and gas pipelines, ACS Sustain. Chem. Eng. 11 (2023) 353–367, https://doi.org/10.1021/acssuschemeng.2c05716.
[54] A. Farhadian, Y. Zhao, P. Naeiji, A. Rahimi, A. Berisha, L. Zhang, et al., Simultaneous inhibition of natural gas hydrate formation and CO2/H2S corrosion for flow assurance inside the oil and gas pipelines, Energy 269 (2023), 126797, https://doi.org/10.1016/J.ENERGY.2023.126797.
[55] R. Haldhar, C. Jayprakash Raorane, V.K. Mishra, T. Periyasamy, A. Berisha, S.C. Kim, Development of different chain lengths ionic liquids as green corrosion inhibitors for oil and gas industries: experimental and theoretical investigations, J. Mol. Liq. 372 (2023), 121168, https://doi.org/10.1016/J.MOLLIQ.2022.121168.
[56] D. Iravani, N. Esmaeili, A. Berisha, E. Akbarinezhad, M.H. Aliabadi, The quaternary ammonium salts as corrosion inhibitors for X65 carbon steel under sour environment in NACE 1D182 solution: experimental and computational studies, Colloids Surf. A Physicochem. Eng. Asp. 656 (2023), 130544, https://doi.org/10.1016/j.colsurfa.2022.130544.
[57] A. Dabagh, A. Bagui, M. Abali, R. Aziam, M. Chiban, F. Sinan, et al., Increasing the adsorption efficiency of methylene blue by acid treatment of the plant Carpobrotus edulis, Chem Afr 4 (2021) 585–598, https://doi.org/10.1007/s42250-021-00233-z.
[58] A. Dabagh, R. Benhiti, M. Abali, A. Ait Ichou, F. Sinan, M. Zerbet, Valorization of plant biomass by chemical pretreatment: application to the removal of Rhodamine B and Congo Red dyes, Biomass Convers Biorefinery (2023), https://doi.org/10.1007/s13399-023-04299-2.
[59] M. Shirani, A. Semnani, H. Haddadi, S. Habibollahi, Optimization of simultaneous removal of methylene blue, crystal violet, and fuchsine from aqueous solutions by magnetic NaY zeolite composite, Water Air Soil Pollut. 225 (2014) 1–15.
[60] A. Thakur, H. Kaur, Response surface optimization of Rhodamine B dye removal using paper industry waste as adsorbent, Int J Ind Chem 8 (2017) 175–186.
[61] M.A.M. Salleh, D.K. Mahmoud, W.A.W.A. Karim, A. Idris, Cationic and anionic dye adsorption by agricultural solid wastes: a comprehensive review, Desalination 280 (2011) 1–13, https://doi.org/10.1016/j.desal.2011.07.019.
[62] M.H. Cetin, B. Ozcelik, E. Kuram, E. Demirbas, Evaluation of vegetable based cutting fluids with extreme pressure and cutting parameters in turning of AISI 304L by Taguchi method, J. Clean. Prod. 19 (2011) 2049–2056.
[63] S. Ajebli, G. Kaichouh, M. Khachani, H. Babas, M. EL Karbane, Z.S. Safi, et al., Modeling of tenofovir disoproxil fumarate decontamination using sodium alginate-encapsulated activated carbon: molecular dynamics, Monte Carlo and density functional theory, Colloids Surf. A Physicochem. Eng. Asp. 663 (2023), 131057, https://doi.org/10.1016/J.COLSURFA.2023.131057.
[64] M. Sadiku, T. Selimi, A. Berisha, A. Maloku, V. Mehmeti, V. Thaçi, et al., Removal of methyl violet from aqueous solution by adsorption onto halloysite nanoclay: experiment and theory, Toxics 10 (2022) 445, https://doi.org/10.3390/TOXICS10080445, 2022;10:445.
[65] O. Amrhar, M. Mobarak, A. Berisha, M.S. Elyoubi, H. Nassali, Natural illitic clay as an eco-friendly adsorbent for removal of Cu (II) ions from aqueous solution: experimental study, data modeling, and Monte Carlo simulation, Biointerface Res Appl Chem 13 (2023), https://doi.org/10.33263/BRIAC136.535.
[66] A. Berisha, First principles details into the grafting of aryl radicals onto the free-standing and borophene/Ag(1 1 1) surfaces, Chem. Phys. 544 (2021), 111124, https://doi.org/10.1016/j.chemphys.2021.111124.
[67] L. El Hammari, R. Hamed, K. Azzaoui, S. Jodeh, S. Latifi, S. Saoiabi, et al., Optimization of the adsorption of lead (II) by hydroxyapatite using a factorial design: density functional theory and molecular dynamics, Front. Environ. Sci. 11 (2023) 244.
[68] J. El Gaayda, F. Ezzahra Titchou, R. Oukhrib, I. Karmal, H. Abou Oualid, A. Berisha, et al., Removal of cationic dye from coloured water by adsorption onto hematite-humic acid composite: experimental and theoretical studies, Sep. Purif. Technol. 288 (2022), 120607, https://doi.org/10.1016/j.seppur.2022.120607.
[69] H.A. Rub, A. Deghles, O. Hamed, K. Azzaoui, B. Hammouti, M. Taleb, et al., Cellulose based polyurethane with amino acid functionality: design, synthesis, computational study and application in wastewater purification, Int. J. Biol. Macromol. 239 (2023), https://doi.org/10.1016/j.ijbiomac.2023.124328.
[70] A. Berisha, Interactions between the arylдiazonium cations and graphene oxide: a DFT study, J. Chem. 2019 (2019), https://doi.org/10.1155/2019/5126071.
[71] H. Jafari, E. Ameri, F. Soltanolkottabi, A. Berisha, M. Seydou, Experimental and theoretical investigations of new Schiff base compound adsorption on aluminium in 1 M HCl, J. Electrochem. Sci. Eng. 12 (2022) 975–987, https://doi.org/10.5599/jese.1405.
[72] A. Dabagh, M. Abali, A. Ait Ichou, R. Benhiti, F. Sinan, M. Zerbet, Optimization and modeling of adsorption of Congo Red and Rhodamine B dyes onto Carpobrotus edulis plant, J Dispers Sci Technol (2022) 1–10.